

Invariant Stochastic Encoders*

Stephen Luttrell

June 28, 2018

Abstract: The theory of stochastic vector quantisers (SVQ) has been extended to allow the quantiser to develop invariances, so that only "large" degrees of freedom in the input vector are represented in the code. This has been applied to the problem of encoding data vectors which are a superposition of a "large" jammer and a "small" signal, so that only the jammer is represented in the code. This allows the jammer to be subtracted from the total input vector (i.e. the jammer is nulled), leaving a residual that contains only the underlying signal. The main advantage of this approach to jammer nulling is that little prior knowledge of the jammer is assumed, because these properties are automatically discovered by the SVQ as it is trained on examples of input vectors.

1 Introduction

In vector quantisation a code book is used to encode each input vector as a corresponding code index, which is then decoded (again, using the codebook) to produce an approximate reconstruction of the original input vector [1, 2]. The standard approach to vector quantiser (VQ) design [3] may be generalised [4] so that each input vector is encoded as a *vector* of code indices that are stochastically sampled from a probability distribution that depends on the input vector, rather than as a *single* code index that is the deterministic outcome of finding which entry in a code book is closest to the input vector. This will be called a stochastic VQ (SVQ), and it includes the standard VQ as a special case.

One advantage of using the stochastic approach is that it automates the process of splitting high-dimensional input vectors into low-dimensional blocks before encoding them, because minimising the mean Euclidean reconstruction error can encourage different stochastically sampled code indices to become associated with different input subspaces [5, 6]. Another advantage is that it is very easy to connect SVQs together, by using the vector of code index probabilities computed by one SVQ as the input vector to another SVQ [7].

SVQ theory will be extended to the case of encoding noisy (or distorted) data, with the intention of subsequently reconstructing an approximation to

*Full version of a short paper that was published in the Digest of the 5th IMA International Conference on Mathematics in Signal Processing, 18-20 December 2000, Warwick University, UK.

the noiseless data. This theory is then applied to the problem of encoding data vectors which are a superposition of a "large" jammer and a "small" signal, where the signal is regarded as a distortion superimposed on the jammer, rather than the other way around. The reconstruction is then an approximation to the jammer, which can thus be subtracted from the original data to reveal the underlying signal of interest.

In Section 2 the underlying theory of SVQs is developed together with its extension to the encoding of noisy data, and in Section 3 some simulations illustrating the application of SVQs to the nulling of jammers are presented.

2 Stochastic Vector Quantiser Theory

In Section 2.1 the basic theory of folded Markov chains (FMC) is given [8], in Section 2.2 FMC theory is extended to the case of encoding noisy or distorted data with the intention of eventually recovering the undistorted data, in Section 2.3 this extended theory is applied to the problem of encoding data that contain unwanted "nuisance degrees of freedom", in Section 2.4 some constraints (including the threshold trick of [9]) on the optimisation of the encoder are introduced to encourage the encoder to disregard the nuisance degrees of freedom (i.e. discover invariances), and finally in Section 2.5 this invariant encoder theory is applied to the problem of encoding and subsequently nulling "large" jammers that obscure "small" signals.

2.1 Folded Markov Chains

The basic building block of the SVQ used in this paper is the folded Markov chain (FMC) [8]. An input vector x is encoded as a code index vector y , which is then subsequently decoded as a reconstruction x' of the input vector. Both the encoding and decoding operations are allowed to be probabilistic, in the sense that y is a sample drawn from $\Pr(y|x)$, and x' is a sample drawn from $\Pr(x'|y)$, where $\Pr(y|x)$ and $\Pr(x'|y)$ are Bayes' inverses of each other, as given by $\Pr(x'|y) = \frac{\Pr(y|x)\Pr(x)}{\int dz \Pr(y|z)\Pr(z)}$, and $\Pr(x)$ is the prior probability from which x is sampled.

In order to ensure that the FMC encodes the input vector optimally, a measure of the reconstruction error must be minimised. There are many possible ways to define this measure, but one that is consistent with many previous results, and which also leads to many new results, is the mean Euclidean reconstruction error measure D , which is defined as [8]

$$D \equiv \int dx \Pr(x) \sum_{y_1=1}^M \sum_{y_2=1}^M \cdots \sum_{y_n=1}^M \Pr(y|x) \int dx' \Pr(x'|y) \|x - x'\|^2 \quad (1)$$

where $y = (y_1, y_2, \dots, y_n)$, $1 \leq y_i \leq M$ is assumed, $\Pr(x) \Pr(y|x) \Pr(x'|y)$ is the joint probability that the FMC has state (x, y, x') , $\|x - x'\|^2$ is the Euclidean

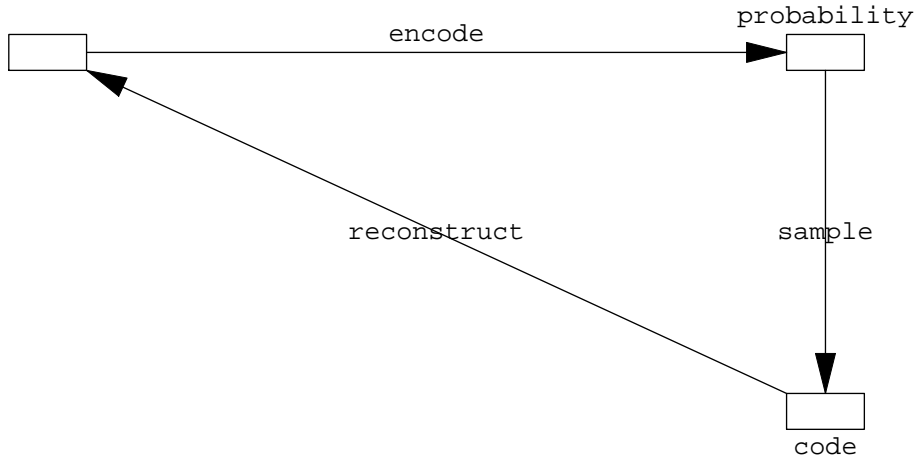


Figure 1: A folded Markov chain (FMC) in which an input vector x is encoded as a code index vector y that is drawn from a conditional probability $\Pr(y|x)$, which is then decoded as a reconstruction vector x' drawn from the Bayes' inverse conditional probability $\Pr(x'|y)$.

reconstruction error, and $\int dx \sum_{y_1=1}^M \sum_{y_2=1}^M \cdots \sum_{y_n=1}^M \int dx'(\cdots)$ sums over all possible states of the FMC (weighted by the joint probability).

The Bayes' inverse probability $\Pr(x'|y)$ may be integrated out of this expression for D to yield [8]

$$D = 2 \int dx \Pr(x) \sum_{y_1=1}^M \sum_{y_2=1}^M \cdots \sum_{y_n=1}^M \Pr(y|x) \|x - x'(y)\|^2 \quad (2)$$

where the reconstruction vector $x'(y)$ is defined as $x'(y) \equiv \int dx \Pr(x|y)x$. Because of the quadratic form of the objective function, it turns out that $x'(y)$ may be treated as a free parameter whose optimum value (i.e. the solution of $\frac{\partial D}{\partial x'(y)} = 0$) is $\int dx \Pr(x|y)x$, as required.

2.2 Noisy Data

The FMC approach can be generalised to the problem of encoding noisy or distorted data, with the intention of eventually recovering the undistorted data. This generalisation is based on the results reported in [10]. The input vector is x_0 , which is converted into the distorted input vector x by a distortion process $\Pr(x|x_0)$, which is then encoded as a code index vector y , which is then subsequently decoded as a reconstruction x'_0 of the original input vector. This is described by the directed graph $x_0 \rightarrow x \rightarrow y \rightarrow x'_0$. The operations that occur are summarised in Figure 2.

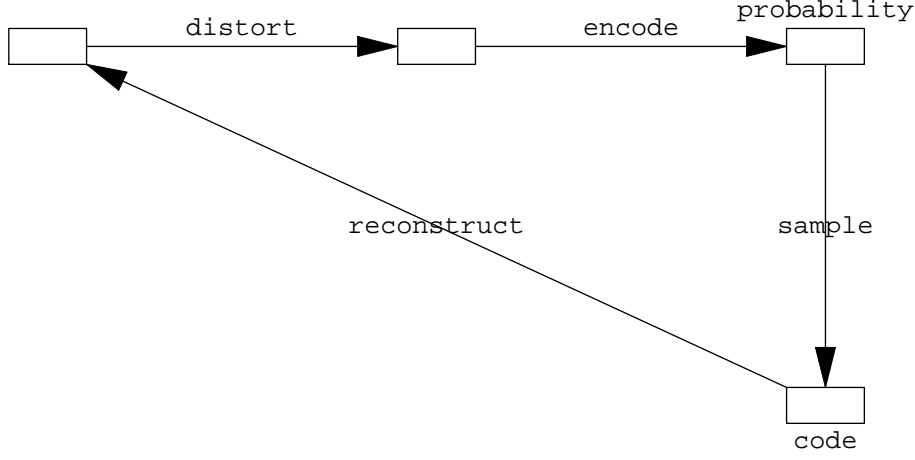


Figure 2: A folded Markov chain (FMC) in which an input vector x_0 is first distorted into x , which is then encoded as a code index vector y that is drawn from a conditional probability $\Pr(y|x)$, which is then decoded as a reconstruction vector x'_0 drawn from the Bayes' inverse conditional probability $\Pr(x'_0|y)$.

The mean Euclidean reconstruction error measure D becomes (compare Equation 1)

$$D = \int dx_0 \Pr(x_0) \int dx \Pr(x|x_0) \sum_{y_1=1}^M \sum_{y_2=1}^M \cdots \sum_{y_n=1}^M \Pr(y|x) \int dx' \Pr(x'_0|y) \|x_0 - x'_0\|^2 \quad (3)$$

The Bayes' inverse probability $\Pr(x'_0|y)$ may be integrated out of this expression for D to yield (compare Equation 2)

$$D = 2 \int dx_0 \Pr(x_0) \int dx \Pr(x|x_0) \sum_{y_1=1}^M \sum_{y_2=1}^M \cdots \sum_{y_n=1}^M \Pr(y|x) \|x_0 - x'_0(y)\|^2 \quad (4)$$

where the reconstruction vector $x'_0(y)$ is defined as $x'_0(y) \equiv \int dx_0 \Pr(x_0|y)x_0$, which may be treated as a free parameter.

Bayes' theorem $\Pr(x_0) \Pr(x|x_0) = \Pr(x) \Pr(x_0|x)$ may be used to integrate out x_0 to yield

$$D = 2 \int dx \Pr(x) \sum_{y_1=1}^M \sum_{y_2=1}^M \cdots \sum_{y_n=1}^M \Pr(y|x) \|x_0(x) - x'_0(y)\|^2 + \text{constant} \quad (5)$$

where $x_0(x)$ is defined as $x_0(x) \equiv \int dx_0 \Pr(x_0|x)x_0$.

It is much more difficult to optimise this version of the objective function than the version in Equation 2, because the $x_0(x)$ term is in general a non-linear

function of x . Worse still, the expression for $x_0(x)$ involves $\Pr(x_0|x)$, which depends on the unknown $\Pr(x_0)$, so $x_0(x)$ cannot be computed analytically anyway. The situation looks irretrievable, but it turns out that some progress can be made by conceptually splitting x into "signal" and "noise" subspaces, as will be shown in Section 2.3.

2.3 Nuisance Degrees of Freedom

For convenience, split up the input space into (possibly non-orthogonal) subspaces as (x_0, x_\perp) , where all of the distortion is contained in x_\perp , which requires that any distortion that lies *in* the x_0 subspace is regarded as part of the undistorted input. The directed graph becomes $(x_0, 0) \rightarrow (x_0, x_\perp) \rightarrow y \rightarrow x'_0$ as shown in Figure 3.

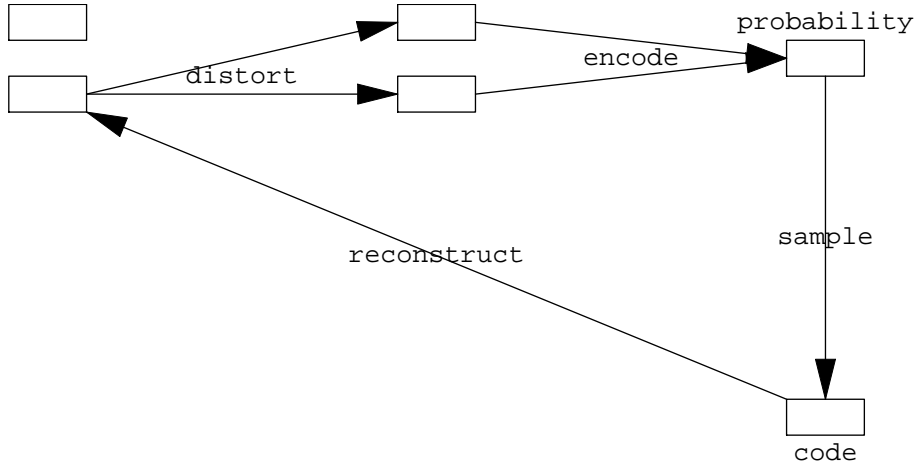


Figure 3: A folded Markov chain (FMC) in which an input vector $(x_0, 0)$ is first distorted into (x_0, x_\perp) , which is then encoded as a code index vector y that is drawn from a conditional probability $\Pr(y|x_0, x_\perp)$, which is then decoded as a reconstruction vector x'_0 drawn from the Bayes' inverse conditional probability $\Pr(x'_0|y)$.

The expression for D becomes (compare Equation 4).

$$D = 2 \int dx_0 \Pr(x_0) \int dx_\perp \Pr(x_\perp|x_0) \sum_{y_1=1}^M \sum_{y_2=1}^M \cdots \sum_{y_n=1}^M \Pr(y|x_0, x_\perp) \|x_0 - x'_0(y)\|^2 \quad (6)$$

Consider the related optimisation problem in which an attempt to to reconstruct (x_0, x_\perp) is made, as shown in Figure 4. The corresponding objective function may be obtained by modifying Equation 6, where the cross-term arising from

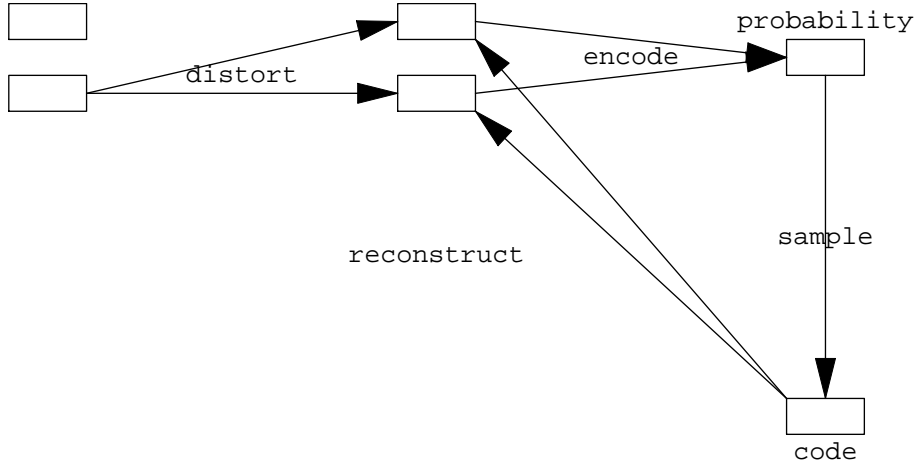


Figure 4: Modified version of Figure 3 in which the reconstruction link is switched from the original undistorted signal to the full signal+distortion.

non-orthogonal (x_0, x_\perp) is omitted.

$$D = 2 \int dx_0 \Pr(x_0) \int dx_\perp \Pr(x_\perp | x_0) \sum_{y_1=1}^M \sum_{y_2=1}^M \cdots \sum_{y_n=1}^M \Pr(y | x_0, x_\perp) \times \left(\|x_0 - x'_0(y)\|^2 + \|x_\perp - x'_\perp(y)\|^2 \right) \quad (7)$$

Assume for now (to be justified below) that some of the links in Figure 4 are broken as shown in Figure 5. Because the distortion subspace is not involved in the computations in Figure 5, it may be redrawn as shown in Figure 6. This is the same as Figure 3, except that the encoder now disregards (or is invariant with respect to) the nuisance degrees of freedom.

In order to break the links as shown in Figure 5 the following argument is required:

1. Assume that the encoder is independent of x_\perp , so that $\Pr(y | x_0, x_\perp) = \Pr(y | x_0)$.
2. The $\|x_\perp - x'_\perp(y)\|^2$ term in D needs to simplify to a constant.
3. This requires that $\int dx_0 \Pr(x_0) \int dx_\perp \Pr(x_\perp | x_0) \sum_{y_1=1}^M \sum_{y_2=1}^M \cdots \sum_{y_n=1}^M \Pr(y | x_0) \|x_\perp - x'_\perp(y)\|^2 = \text{constant}$.
4. To guarantee this constant, it is sufficient to have $\int dx_\perp \Pr(x_\perp | x_0) \|x_\perp - x'_\perp(y)\|^2 = \text{constant}$ independent of x_0 and y .
5. To guarantee this constant independent of x_0 and y , it is sufficient to have $\Pr(x_\perp | x_0) = \Pr(x_\perp)$.

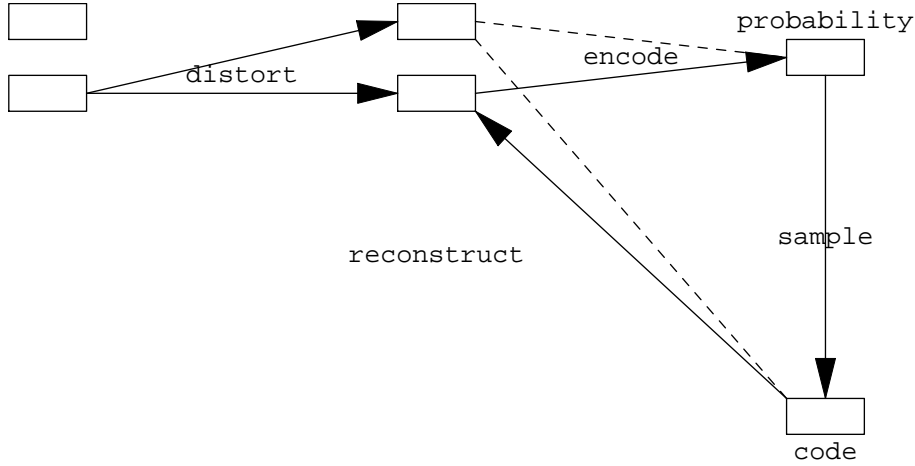


Figure 5: Modified version of Figure 4 in which the encoder (and reconstruction) links from (and to) the distortion subspace are deleted (as indicated by the dashed lines).

6. Given that $\Pr(x_{\perp}|x_0) = \Pr(x_{\perp})$ and $\Pr(y|x_0, x_{\perp}) = \Pr(y|x_0)$, then making the replacement $x'_{\perp}(y) \rightarrow \langle x_{\perp} \rangle$ in D will give an objective function with the same stationary points as D , because $x'_{\perp}(y) = \langle x_{\perp} \rangle$ is the stationary point of D with respect to $x'_{\perp}(y)$.
7. Given that $\Pr(x_{\perp}|x_0) = \Pr(x_{\perp})$ and $x'_{\perp}(y) = \langle x_{\perp} \rangle$, the result $\int dx_{\perp} \Pr(x_{\perp}|x_0) \|x_{\perp} - x'_{\perp}(y)\|^2 = \text{constant}$ independent of x_0 and y follows automatically.

The assumptions may be summarised as

$$\begin{aligned} \Pr(y|x_0, x_{\perp}) &= \Pr(y|x_0) \\ \Pr(x_{\perp}|x_0) &= \Pr(x_{\perp}) \end{aligned} \quad (8)$$

which allow the objective function D (see Equation 7) to be replaced by the equivalent objective function

$$D = 2 \int dx_0 \Pr(x_0) \sum_{y_1=1}^M \sum_{y_2=1}^M \cdots \sum_{y_n=1}^M \Pr(y|x_0) \|x_0 - x'_0(y)\|^2 + \text{constant} \quad (9)$$

This is the standard FMC objective function (compare Equation 2) for encoding and reconstructing the undistorted input, for which the directed graph is $x_0 \rightarrow y \rightarrow x'_0$. Note that, under the stated assumptions, the simplification in Equation 9 occurs even if the two subspaces are not orthogonal to each other, the potential cross-term $\int dx_{\perp} \Pr(x_{\perp}|x_0) (x_0 - x'_0(y)) \cdot (x_{\perp} - x'_{\perp}(y))$ in Equation 7 is zero.

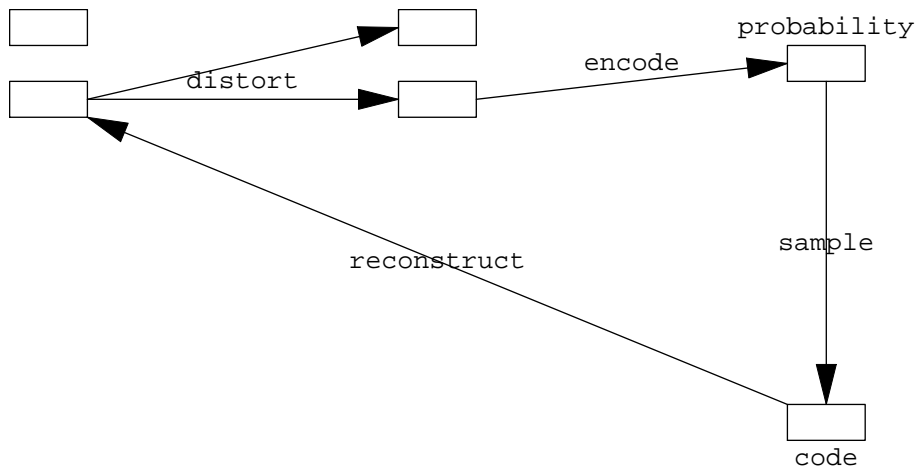


Figure 6: Equivalent version of Figure 5 in which the reconstruction link is moved to an equivalent position.

In summary, the encoder has access only to the signal + distortion (x_0, x_\perp) (see Figure 4 and Equation 7), but the assumptions in Equation 8 force the encoder to disregard the distortion (see Figure 6 and Equation 9). In practice, it is not possible to satisfy these assumptions in general, because it is not known in advance how to extract orthogonal signal and distortion subspaces (x_0, x_\perp) given examples of only the distorted signal. However, these assumptions may be encouraged to hold true by minimising D (as defined in Equation 7) under certain constraints, in which case Figure 6 and Equation 9 follow automatically from Figure 4 and Equation 7, respectively. These constraints are discussed in Section 2.4.

This type of encoder, in which the large degrees of freedom are preferentially encoded, can be used as the basis of a so-called "residual vector quantiser" [11], in which (quoting from [11]) "the quantiser has a sequence of encoding stages, where each stage encodes the residual (error) vector of the prior stage". Note that a residual vector quantiser is a special case of the type of multistage encoder discussed in [7].

2.4 Optimisation Constraints

Henceforth, only the scalar case will be considered, so the vector y is now replaced by the scalar y ($1 \leq y \leq M$). In order to implement a practical optimisation procedure for minimising D it is necessary to introduce a variety of assumptions and constraints.

Because $\Pr(y|x)$ is a probability it satisfies $\Pr(y|x) \geq 0$ and $\sum_{y=1}^M \Pr(y|x) = 1$,

which is guaranteed if $\Pr(y|x)$ is written as

$$\Pr(y|x) = \frac{Q(y|x)}{\sum_{y'=1}^M Q(y'|x)} \quad (10)$$

where $Q(y|x) \geq 0$. This removes the need to explicitly impose the constraint $\sum_{y=1}^M \Pr(y|x) = 1$ during optimisation. The $Q(y|x)$ are the unnormalised *likelihoods* of sampling code index y from the code book.

However, $Q(y|x)$ itself needs to be described by a finite number of parameters in order that the values that minimise $D_1 + D_2$ may be derived from a finite amount of training data. It can be shown that the optimal form of $\Pr(y|x)$ is piecewise linear in x [7], and that for training data that lie on smooth curved manifolds the form of this solution is well approximated by a piecewise linear $Q(y|x)$ of the form [6]

$$Q(y|x) = \begin{cases} w(y).x - a(y) & w(y).x \geq a(y) \\ 0 & w(y).x \leq a(y) \end{cases} \quad (11)$$

which is the same as the functional form used for the neural response in [9]. However, the precise functional form of $Q(y|x)$ needs to exhibit this behaviour only in the vicinity of the data manifold, so in particular it can be allowed to saturate (i.e. $Q(y|x) \rightarrow 1$) as $w(y).x \rightarrow \infty$. A convenient functional form that achieves this is the sigmoid, which is defined as

$$Q(y|x) = \frac{1}{1 + \exp(-w(y).x - b(y))} \quad (12)$$

This reduces the problem of minimising D to one of finding the optimal values of the $w(y)$, $b(y)$ and $x'(y)$. This may be done by using the gradient descent procedure described in [4].

If the input is an *undistorted* signal (i.e. $x = (x_0, 0)$) which lies on a smooth curved manifold, then the sigmoids can cooperate in encoding this input as illustrated in Figure 7, where the sigmoid threshold planes $w(y).x + b(y) = 0$ are shown slicing pieces off the curved manifold [6].

The additional constraints that are required in order to implement the behaviour described in Section 2.3 will now be described. Thus the constraints must be such that the encoder disregards (or is invariant with respect to) the nuisance degrees of freedom x_\perp in the full input vector (x_0, x_\perp) . However, without knowing $\Pr(x_0, x_\perp)$ in advance (which would allow $x_0(x)$ in Equation 5 to be calculated), it is not possible to give a general approach that works in all cases. At best, an empirical approach must be used.

A very simple and useful constraint is to impose a threshold constraint on the sigmoid function, which forces the value of the sigmoid to lie exactly halfway up its slope when the norm of its input vector is θ . This is achieved by choosing

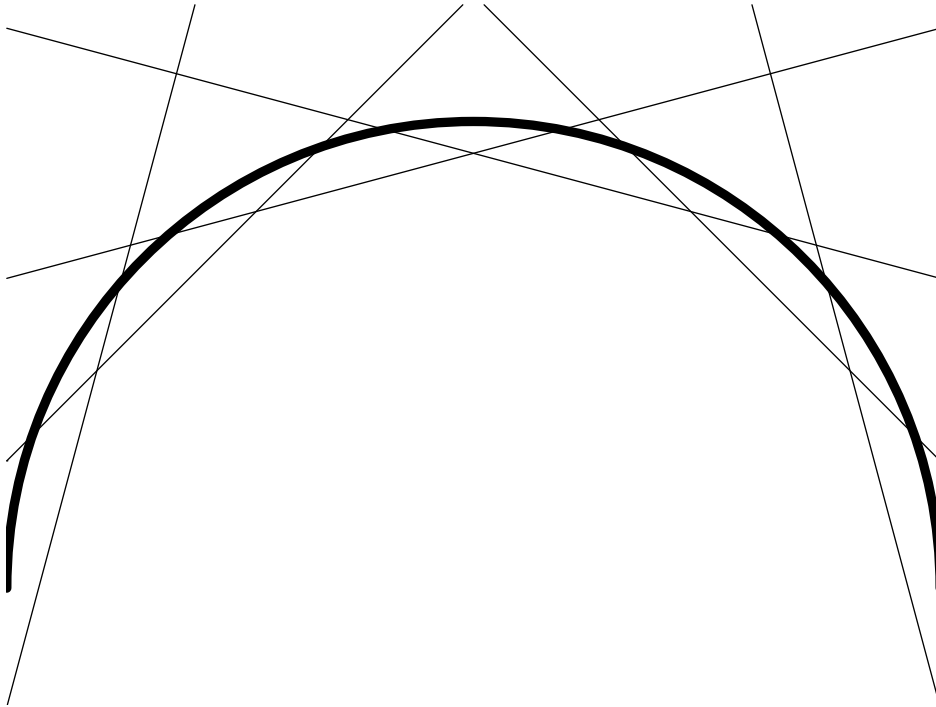


Figure 7: Illustration of how a number of sigmoids can cooperate to slice pieces off a signal manifold.

$b(y) = -\theta|w(y)|$, so that

$$Q(y|x) = \frac{1}{1 + \exp(-(\hat{w}(y) \cdot x - \theta) \|w(y)\|)} \quad (13)$$

where $\|w(y)\| \equiv \sqrt{w(y) \cdot w(y)}$ and $\hat{w}(y) \equiv \frac{w(y)}{\|w(y)\|}$.

If the input is a *distorted* signal (i.e. $x = (x_0, x_\perp)$) which lies on a "thickened" version of the smooth curved manifold of Figure 7 (the thickness represents the nuisance degrees of freedom), then the sigmoids can cooperate in encoding this input as illustrated in Figure 8, where the sigmoid threshold planes $\hat{w}(y) \cdot x = \theta$ are shown slicing pieces off the curved manifold in a way that disregards the nuisance degrees of freedom. Note that in Figure 8 the representation of thickening is not complete, because it can actually occur in *any* direction orthogonal to the manifold, including directions orthogonal to the space in which the manifold is embedded; the radial direction in Figure 8 does not include this latter possibility.

In practice, for numerical efficiency and to encourage the optimisation procedure to locate the global minimum of $D_1 + D_2$, it is useful to introduce two additional constraints. Firstly, because optimal solutions typically satisfy

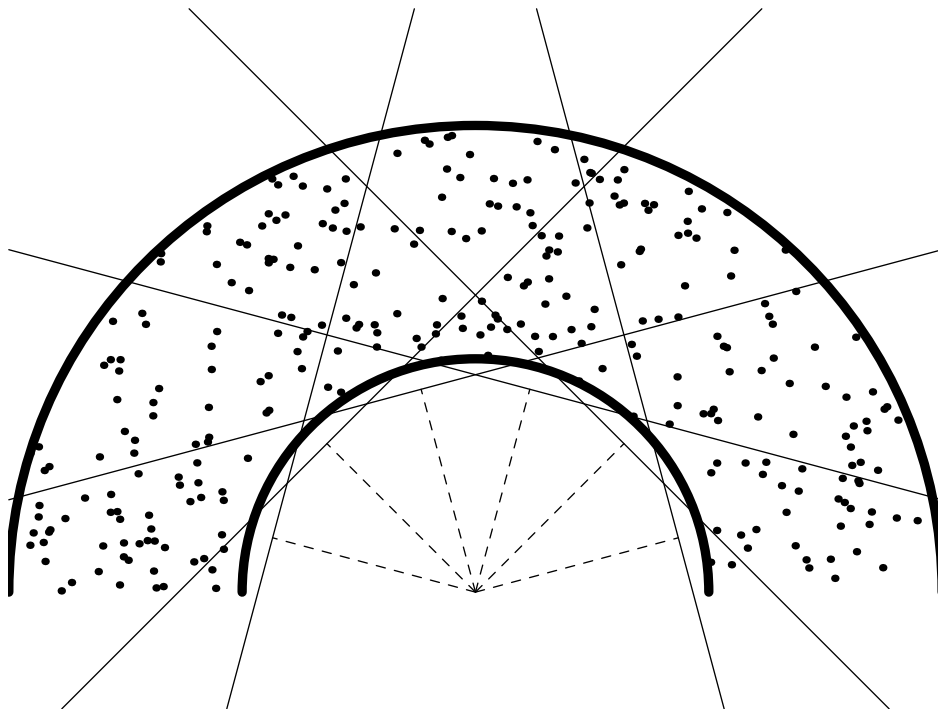


Figure 8: Illustration of how a number of sigmoids can cooperate to slice pieces off a signal manifold thickened by nuisance degrees of freedom.

$x'(y) \approx w(y)$ up to a multiplicative constant, each reconstruction vector $x'(y)$ can be forced to lie parallel to the corresponding weight vector $w(y)$, so that $x'(y) \propto w(y)$; this constraint was also used in [12], but there it was a necessary part of the optimisation procedure, whereas here it merely encourages faster convergence. Secondly, the norm of the weight vectors $\|w(y)\|$ can be constrained as $\|w(y)\| = w_0$, in order to avoid situations where they grow to rather large values which make $Q(y|x)$ (and hence $\Pr(y|x)$) depend very strongly on x in some regions. Both of these constraints speed up convergence to the global minimum of $D_1 + D_2$, can finally be lifted in the vicinity of an optimal solution to obtain complete convergence.

2.5 Jammer Nulling

A number of examples of typical behaviours of $\Pr(y|x)$ are shown in Figure 9.

In Figure 9 the signal and jammer degrees of freedom generate a pair of non-orthogonal subspaces, whose axes are indicated in bold. The response contours of a variety of possible $\Pr(y|x)$ are shown. In the "full" case a pair of $\Pr(y|x)$ respond to the signal and jammer subspaces respectively. In the "signal" case

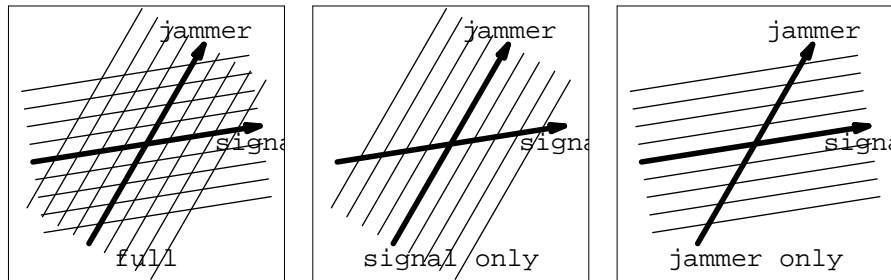


Figure 9: Examples of the response of $\Pr(y|x)$ to signal and jammer subspaces.

a $\Pr(y|x)$ responds to only the signal subspace, and is thus invariant over the jammer subspace. In the "jammer" case the situation is the reverse of the "signal" case. This argument may readily be generalised to any number of $\Pr(y|x)$.

If it is assumed that the jammer is the "large" degree of freedom and the signal is the "small" degree of freedom, the signal and jammer subspaces may be separated by adjusting the threshold parameter θ so that in figure XXX the "jammer" case is obtained, in which case the $\Pr(y|x)$ for $y = 1, 2, \dots, M$ will all become invariant over the signal subspace. The jammer subspace is then spanned by the set of gradient vectors $\nabla \Pr(y|x)$ for $y = 1, 2, \dots, M$, which can thus be used to construct a projection operator J onto the jammer subspace, and a projection operator $1 - J$ onto the signal subspace. This definition of the projection operator may also be used in cases where the jammer and signal subspaces are curved, so that the directions of their axes are functions of x , and all of the straight lines in Figure 9 are replaced by curves defining a curvilinear coordinate system and its coordinate surfaces. Note that curved subspaces are the norm rather than the exception.

3 Jammer Nulling Simulations

The optimisation of the encoder may be done by minimising D using gradient descent [4], using the sigmoid function in Equation 13 to constrain the optimisation so that it encodes only the jammer subspace.

In these simulations the input vector x is 100-dimensional so that $x = (x_1, x_2, \dots, x_{100})$, and each vector in the training set is independently generated as a superposition of a pair of response functions

$$x_i = a_s \frac{\sin\left(\frac{i-i_s}{\sigma}\right)}{\frac{i-i_s}{\sigma}} + a_j \frac{\sin\left(\frac{i-i_j}{\sigma}\right)}{\frac{i-i_j}{\sigma}} \quad (14)$$

where a_s is the signal amplitude that is uniformly distributed in the interval $[-\sqrt{10^{-3}}, \sqrt{10^{-3}}]$ (this corresponds to a signal level of -30dB), a_j is the jammer

amplitude that is uniformly distributed in the interval $[-1, 1]$ (this corresponds to a jammer level of 0dB), i_s is the signal location that is chosen to be 50, i_j is the jammer location that is uniformly distributed in the interval $[38 - \Delta, 38 + \Delta]$ ($\Delta = 0, 2, 4$ is used in the simulations), and σ is the width of the response function that is chosen to be 2. The peak and the first zero of the sinc function are separated by $\pi\sigma$, which defines the resolution cell size. The mean jammer position and the signal position satisfy $i_s - \langle i_j \rangle = 12$, which corresponds to a separation of $\frac{12}{\pi\sigma} \approx 2$ resolution cells. Random noise uniformly distributed in the interval $[-\sqrt{10^{-5}}, \sqrt{10^{-5}}]$ (this corresponds to a noise level of -50dB) is also added to each component of the training vector.

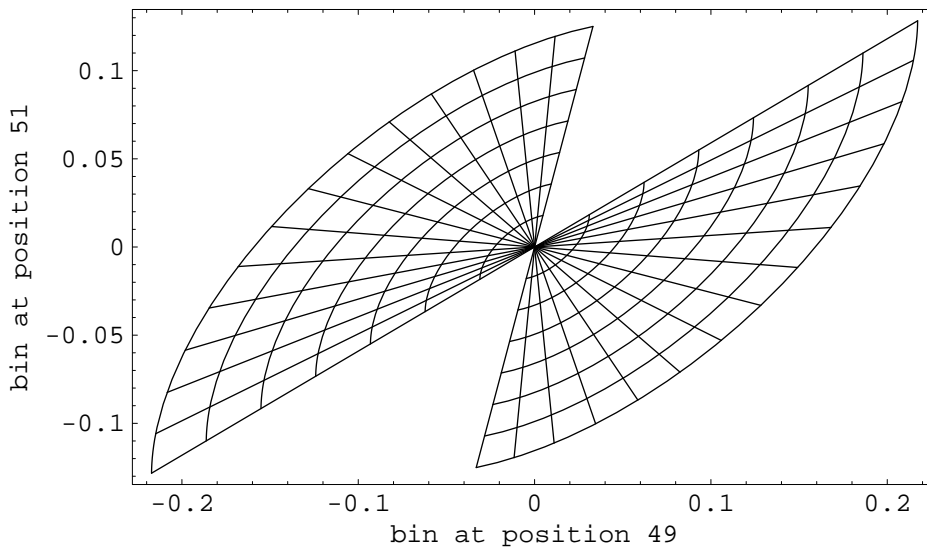


Figure 10: A two-dimensional projection of the curved manifold generated by the jammer when $\Delta = 2$.

In Figure 10 the 2-dimensional manifold generated by varying the jammer position over the interval $[38 - \Delta, 38 + \Delta]$ (for $\Delta = 2$), and varying the jammer amplitude over the interval $[-1, 1]$, is shown. Because the input vector x is 100-dimensional, only a low-dimensional projection can be visualised, and the 2-dimensional vector (x_{49}, x_{51}) is displayed here. The curvilinear grid traces out the coordinate surfaces of jammer position i_j and jammer amplitude a_j , and the whole diagram shows how this grid is embedded in (x_{49}, x_{51}) -space. Note that the a_j dimension behaves as a "radial" coordinate (straight lines), whereas the i_j dimension behaves as an "angular" coordinate (curved lines).

In Figure 11 an encoder is trained on three different jammer scenarios $\Delta = 0, 2, 4$. After training the encoder is tested for how well it can be used to null a pure jammer (i.e. with no signal or noise added), where the degree

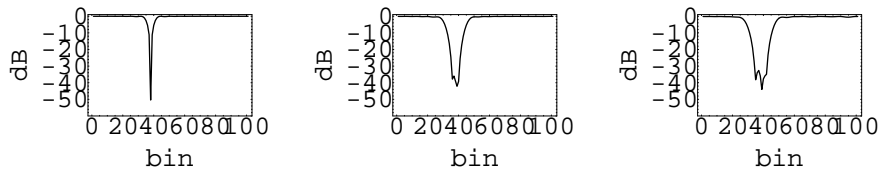


Figure 11: Plot of degree of nulling against nominal jammer location, for jammer locations that are spread over the intervals $[38, 38]$ using $M = 2$, $[36, 40]$ using $M = 4$, and $[34, 42]$ using $M = 6$.

of nulling is defined as the ratio of the squared lengths of the nulled input vector and the original input vector. This is a good test of the ability of the encoder to simultaneously learn the profile of the jammer and the shape of the jammer manifold which is generated by sweeping this profile over the interval $[38 - \Delta, 38 + \Delta]$. When $\Delta = 0$ there is a sharp minimum at the jammer location $i_j = 38$, as expected. When $\Delta = 2$ the minimum becomes spread over the jammer locations $i_j \in [36, 40]$, and when $\Delta = 4$ the minimum becomes spread even more broadly over the jammer locations $i_j \in [34, 42]$. All of these results are as expected.

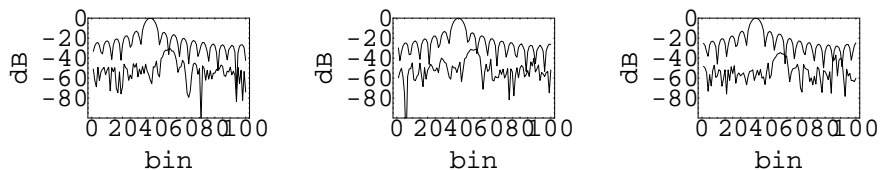


Figure 12: Plot of a typical input vector before and after jammer nulling for each of the scenarios in Figure 11.

In Figure 12 typical examples of an input vector together with how it appears after jammer nulling are shown for each of the jammer scenarios considered in Figure 11. In every case the signal is clearly revealed at its correct location after nulling the jammer.

In all of these training scenarios, one could envisage further constraining some of the properties of the encoder, in order to introduce prior knowledge of the form of the jammer and/or signal subspaces, and to thereby reduce the computational complexity of the jammer nulling. For instance, the signal subspace could be predefined, as in conventional algorithms which hold constant the response in a predefined "look direction". Similarly, the jammer subspace could be built out of predefined subspaces which are optimised so as to maximally null the jammer(s), as in conventional algorithms in which a number of jammer "templates" are used to remove the jammer(s). In general, by choosing appro-

appropriate additional constraints, the SVQ approach to jammer nulling can be made backwardly compatible with conventional approaches.

4 Conclusions

The theory of stochastic vector quantisers (SVQ) [4] has been extended to allow the quantiser to develop invariances, so that only "large" degrees of freedom in the input vector are represented in the code. This has been applied to the problem of encoding data vectors which are a superposition of a "large" jammer and a "small" signal, so that only the jammer is represented in the code. This allows the jammer to be subtracted from the total input vector (i.e. the jammer is nulled), leaving a residual that contains only the underlying signal. Several numerical simulations have shown how that idea works in practice, even when the jammer location is uncertain so that the jammer subspace is curved.

The main advantage of this approach to jammer nulling is that little prior knowledge of the jammer is assumed, because these properties are automatically discovered by the SVQ as it is trained on examples of input vectors. Provided that the signal is much weaker than the jammer, the SVQ acquires an internal representation of the jammer and signal manifolds, in which its code is invariant with respect to the signal. In a sense, the SVQ regards the "large" jammer as the normal type of input that it expects to receive, whereas it regards the "small" signal as an anomaly.

References

- [1] Gray, R. M. (April 1984). *Vector quantisation*. *IEEE Acoust., Speech, Signal Processing Mag.*, 4–29.
- [2] Gersho, A., & Gray, R. M. (1992). *Vector quantisation and signal processing*. Kluwer.
- [3] Linde, Y., Buzo, A., & Gray, R. M. (1980). *An algorithm for vector quantiser design*. *IEEE Trans. COM*, **28**(1), 84–95.
- [4] Luttrell, S. P. (1997). *A theory of self-organising neural networks*. In S. W. Ellacott, J. C. Mason & I. J. Anderson (Ed.), *Mathematics of Neural Networks: Models, Algorithms and Applications* (pp. 240–244). Kluwer.
- [5] Luttrell, S. P. (1997). *Self-organisation of multiple winner-take-all neural networks*. *Connection Science (special issue on Combining Artificial Neural Nets: Modular Approaches)*, **9**(1), 11–30.
- [6] Luttrell, S. P. (1999). *Self-organised modular neural networks for encoding data*. In A. J. Sharkey (Ed.), *Combining Artificial Neural Nets: Ensemble and Modular Multi-Net Systems* (pp. 235–263). Springer-Verlag.

- [7] Luttrell, S. P. (1999). *An adaptive network for encoding data using piecewise linear functions*. In *Proceedings of the 9th International Conference on Artificial Neural Networks (ICANN99)* (pp. 198–203). Edinburgh.
- [8] Luttrell, S. P. (1994). *A Bayesian analysis of self-organising maps*. *Neural Computation*, **6**(5), 767–794.
- [9] Webber, C. J. (1994). *Self-organisation of transformation-invariant detectors for constituents of perceptual patterns*. *Network: Computation in Neural Systems*, **5**(4), 471–496.
- [10] Ephraim, Y., & Gray, R. M. (1988). *A unified approach for encoding clean and noisy sources by means of waveform and autoregressive model vector quantisation*. *IEEE Trans. IT*, **34**(4), 826–834.
- [11] Barnes, C. F., Rizvi, S. A., & Nasrabadi, N. M. (1996). *Advances in residual vector quantisation: a review*. *IEEE Trans. Image Process.*, **5**(2), 226–262.
- [12] Webber, C. J. (1998). *Emergent componential coding of a handwriting-image database by neural self-organisation*. *Network: Computation in Neural Systems*, **9**(4), 433–447.